Proceedings of OMAE2005
24th International Conference on Offshore Mechanics and Arctic Engineering (OMAE 2005)
June 12-17, 2005, Halkidiki, Greece

OMAE2005-67238

MODELING VORTEX INDUCED MOTIONS OF SPARS IN UNIFORM AND STRATIFIED FLOWS

Owen H. Oakley, Jr.
ChevronTexaco

Yiannis Constantinides
ChevronTexaco

Claudia Navarro
Applied Research Associates, Inc.

Samuel Holmes
Applied Research Associates, Inc.

ABSTRACT

This paper examines the vortex induced motions (VIM) of a spar type floating production platform in uniform and sheared currents. The large draft of modern production platforms means that in some of the extreme current events the flow past the platform is highly non-uniform along the hull. We discuss the simulation of these stratified flows associated with hurricane events and loop currents and the implications for experiments and numerical simulations. Model testing options are reviewed along with the potential effects of buoyancy due to temperature and salinity variations in the current. Comparisons are made between experimental test results and numerical simulations of VIM at small scale and projections are made to full scale behavior using computational fluid dynamics (CFD) and detached eddy simulation (DES).

INTRODUCTION

Spar platforms have become an important design type for offshore deepwater operations. The typical spar platform is a long vertical cylinder about 40m in diameter with a draft of 200m, tethered to the ocean floor with a catenary mooring system. Having a small waterplane area compared to its displacement and a low center of gravity, the spar has excellent stability and exhibits small responses to waves. Unfortunately the spar shape is prone to vortex shedding in strong currents which can give rise to large horizontal plane motions - stressing the mooring system and risers. Because vortex shedding is expected in many if not all spar installations, the industry has devised methods to reduce vortex induced motions (VIM) to acceptable levels. The two main approaches are to use strakes to break up the coherence of vortex shedding along the length of the spar and the tuning of the mooring system to keep the natural frequencies of the spar away from the vortex shedding frequencies. Both methods depend on accurate prediction of the flow around the platform. There are two types of current events that govern this aspect of the design: a deep eddy or loop current and a hurricane inertial current. The loop current can reach the full platform depth and is often modeled as a high speed uniform current. The speed of a hurricane current can be somewhat higher than that of a loop current, but the hurricane current is typically shallower and confined to the upper third of the spar platform. Although the VIM might be expected to be smaller in this case, the combined action of the VIM, hurricane generated waves and high mooring line tensions make this an important design condition. At this time there is little full scale data on spar VIM under these conditions and there are many different current and hull design scenarios. Furthermore, neither numerical simulation nor tow tank test procedures are validated for sheared currents. Thus, our objective here is to develop effective predictive capabilities, both numerical and experimental.

In the remainder of this paper we first examine some important aspects of the flow around spar platforms and how these might affect CFD simulations and model scale experiments. At issue are the large size and complex spar geometry of the spar and the nature of sheared currents. Size and geometry affect CFD problem size. Spar platforms are not streamlined cylinders but typically have strakes to reduce VIM and often have external pipes and mooring chains or “appurtenances” which can affect the flow near the platform. The detached nature of the flow, the high Reynolds number and complex geometry suggest very large CFD problem size, stressing computer resources. We investigate the problem of simulation from a practical point of view with regard to the computer resources, the time required and the effect of mesh refinement.

A second concern is the nature of the sheared currents which are the focus of this paper. These currents are associated with density or buoyancy variations which are essential to the maintenance of the current. An important question is the effect of these variations in buoyancy on the flow around the platform. In particular, do these variations need to be simulated in model scale experiments? We first examine the governing equations to see how these currents can be modeled. We then examine the effects of buoyancy by simulating a full scale platform in a sheared current including buoyancy effects. We also examine the potential benefit of artificially inducing sheared currents in scale model experiments in a test basin.

NOMENCLATURE

a = motion amplitude [m]
C_p = specific heat [J/kg-K]
$\sigma, C_{b1}, C_{b2}, C_{wl}, C_{des}$ - Turbulence model constants
D = spar hull diameter [m]
f_s = vortex shedding frequency [Hz]
k_s = roughness height
Q = heat generation per unit volume [J/m^{3}s]
P' = pressure [Pa]
$Re = UL/\nu$ = Reynolds number
S = vorticity magnitude
$\tilde{S}$ = S-A production term
$S_t = Df_s/D$ = Strouhal number
T_n = spar natural sway period in calm water [s]
T = temperature [K]
t = time [s]
u = velocity vector [m/s]
U = current velocity; maximum for sheared profile [m/s]
$U_{rn} = U\ T_n/D$ = nominal reduced velocity
y^+ = dimensionless distance to wall
Δ_e = element characteristic dimension
β = thermal expansion coefficient /C
κ = effective diffusivity [m^2/s]
μ = dynamic viscosity [Pa-s]
Θ = dimensionless temperature
ρ = density [kg/m^3]
τ = stress tensor [Pa]
$\nu, \tilde{\nu}, \chi$ = dummy eddy viscosity variables

$$\frac{D}{Dt} = \frac{\partial}{\partial t} + u \cdot \nabla$$

CFD MODELING OF SPARS WITH COMPLEX GEOMETRIES

Since the installation of the first spar in the Gulf of Mexico [1], the hull shapes have evolved from the "classic" cylinder shape to include "cell" and "truss" configurations [2]. All of these are potentially subject to VIM. Some of these platforms have experienced occurrences of VIM in high currents with amplitudes greater than anticipated during the design. An example of the classic spar is the Genesis platform located in 2,600 feet of water in Green Canyon 20 (see Figure 1). The Genesis design has been examined with extensive model basin experiments and thus is a good candidate for comparison with CFD analyses.

The traditional tool for design has been to perform scale model experiments in a towing tank, basin or flume. This has the advantages of being a physical test. Furthermore, quite detailed models can be built, limited only by the patience and skill of the model builder as seen in the example in Figure 2. Such details are normally included in model scale experiments, including the benchmark tests reported here. On the other hand, model tests have a number of potentially serious shortcomings. Typical model scale factors are on the order of 1:40 or greater so the Reynolds number of the model test is quite different from that of the full scale spar if Froude scaling is used. An additional disadvantage of the model test is the difficulty in getting detailed flow data around the platform to help evaluate

Figure 1 Genesis spar platform under construction showing some of the exterior appurtenances.

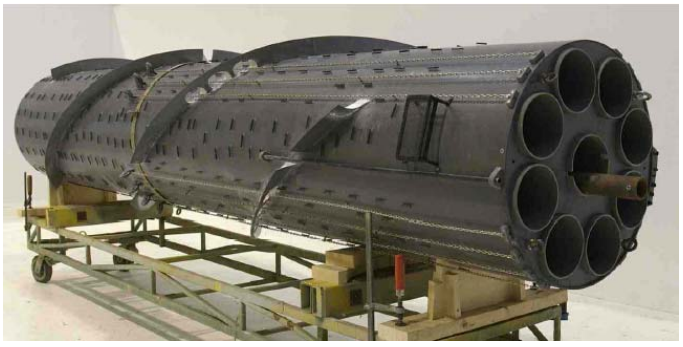

Figure 2 View from of scale model of Genesis hull as tested. The top of spar is on the right. Note strake, pipe, chain and anode details. The scale factor is 1:46.

design changes. Although gross behavior is easily measured, the flow patterns for the unsteady separated flows around the model are not. Another issue is the effect of surface roughness over the wide range of Reynolds numbers from model scale to

full scale. Model tests conducted in a flume or basin typically have turbulent inflow greater than experienced in tanks where the model is towed in quiescent water or in the open sea. The prospect of being able to perform numerical modeling at full scale Reynolds numbers is therefore very attractive.

CFD Modeling

The CFD solver AcuSolve™ was used to obtain approximate solutions of the incompressible Navier-Stokes equations with buoyancy effects. The equations solved that express the conservation of mass, momentum and energy respectively and with z as the vertical axis are:

$$\nabla \cdot u = 0 \tag{1}$$

$$\frac{Du}{Dt} = -\frac{1}{\rho}(\nabla P - \nabla \cdot \tau) + g_z(1 + \beta \Delta T) \tag{2}$$

$$\frac{DT}{Dt} = \nabla \cdot \kappa \nabla T \tag{3}$$

where the dependent variables $P', u, T,$ etc. are locally averaged quantities and κ is the effective diffusivity. Also, for the problem solved here, the stresses τ include turbulent Reynolds stresses. Note that buoyancy effects are included using the Boussinesq approximation in which the changes in density are ignored except for the inclusion of a body force term in the momentum equation. The free surface can be modeled as a free slip rigid surface because the spar motions are at a low Froude number.

Turbulence was modeled using Spalart's version of detached eddy simulation (DES). This DES model is based on the one-equation turbulence model of Spalart-Allmaras [3] so that the change in eddy viscosity is governed by the relation

$$\frac{D\tilde{\nu}}{Dt} = C_{b1}\tilde{S}\tilde{\nu} + \frac{1}{\sigma}(\nabla \cdot ((\nu + \tilde{\nu})\nabla \tilde{\nu}) + C_{b2}(\nabla \tilde{\nu})^2) - C_{w1} f_w \left(\frac{\tilde{\nu}}{d}\right)^2$$

where $\tilde{\nu}$ is a working variable used to obtain the eddy viscosity.

$$\nu_t = \tilde{\nu} f_{\upsilon 1} \; ; \qquad f_{\upsilon 1} = \frac{\chi^3}{\chi^3 + C_{\nu 1}^3} \; ; \qquad \chi = \frac{\tilde{\nu}}{\nu}$$

The constants $\sigma, C_{b1}, C_{b2}, C_{wl}$ are as defined in [3]. The DES turbulence model is obtained by replacing the distance to the wall d with the minimum of the distance to the wall and a measure of the element size ($C_{des}\Delta_e$). Near the wall the model acts like the S-A Reynolds averaged Navier Stokes (RANS) model while far from the wall it behaves as a large eddy simulation (LES) model. As implemented in AcuSolve™, DES transitions smoothly from RANS to LES configurations. The constants required are not given here but are those suggested by Spalart. It should be noted that a feature of this turbulence model is that, at points away from the wall, unresolved (subgrid scale) turbulence is assumed to be isotropic and the eddy viscosity is a function of element size. A danger at the high Re of the problems solved here is that this last assumption is not met.

We used wall functions to describe the flow at the wall in all CFD simulations. This was done to economize on mesh size, but also because both model tests and the full scale spar have rough surfaces. Wall functions reduce mesh size by providing an integrated relationship between the wall and the logarithmic region of the boundary layer. Thus the velocity near the wall is given by:

$$u^+ = \frac{1}{\kappa_w}\ln\left(\frac{y}{k_s}\right) + B$$

where u is the tangential velocity, κ_w and B are constants, k_s is the surface roughness, and y is the distance to the wall. The wall function only makes sense in the region above the surface roughness or when y/k_s is greater than one [4].

All of the solutions shown here were produced using the AcuSolve™ finite element CFD solver. AcuSolve is based on the Galerkin/Least Squares formulation and supports a variety of element types. AcuSolve uses a fully coupled pressure/velocity iterative solver plus a generalized alpha method as a semi-discrete time stepping algorithm. AcuSolve is second order accurate in space and time [5].

The meshes used here were designed to place the first nodes away from the wall just above the surface roughness. In this application, k_s is quite large relative to diameter so the use of wall functions reduces problem size significantly. On the other hand, this type of mesh also tends to produce average calculated values of y^+ to the first node on the order of 20 with maximum values sometimes approaching 100, or larger than usually recommended for smooth cylinders. At this time the alternative is to model the surface roughness explicitly which would be cost prohibitive.

The general mesh strategy was to mesh the boundary layer on the spar and appurtenances with wedge elements and the rest of the flow with tetrahedral or pyramid elements. From a solution point of view, the mesh can be converted to all tetrahedral elements with the same nodes and provide the same solution. We purposely tried to limit the mesh size to less than 2M nodes (near the maximum problem that will fit on our current computer) and to provide reasonable run times. Typical run times for 1500 time steps on a 14 CPU Linux P4 cluster using a gigabit switch are on the order of 50 hours. Run time varies directly with the number of time steps and inversely with time step size and is roughly proportional to the number of nodes in the mesh.

Several different basic meshes simulating the Genesis spar were used in this study. Within each type, a new mesh was generated in order to change the current heading. The first meshes were of a 1:46 scale Genesis model with geometrically

detailed strakes but without any attempt to model external appurtenances. An external view of a typical mesh is shown in Figure 3. Note that the mesh simulates flow in a tank and includes mesh refinement around the spar model and in the wake.

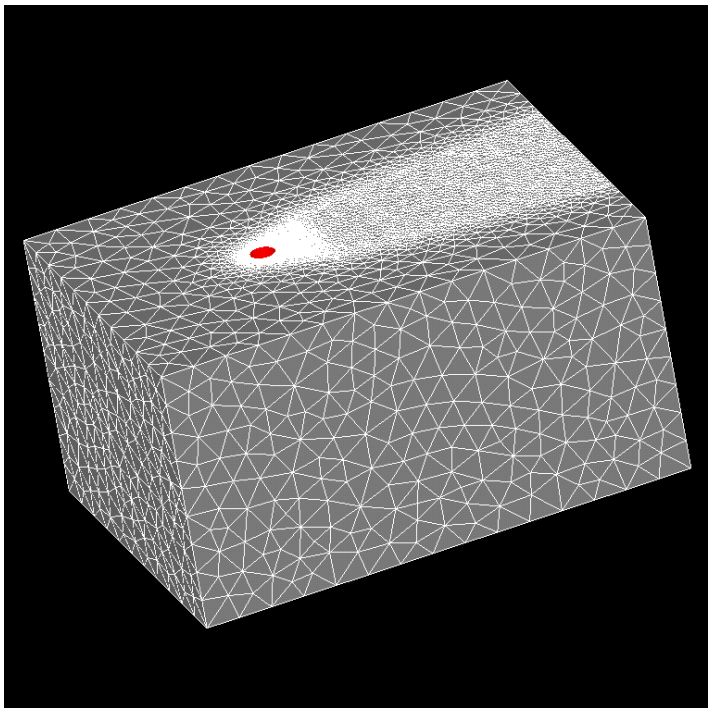

Figure 3 Surface mesh on exterior of fluid domain

The remaining meshes included detailed meshes of a 1:46 scale Genesis model with strakes and appurtenances at several headings, a mesh of a 1:46 scale Genesis model with appurtenances in a basin with a horizontal plate separating the upper and lower regions of the tank and a mesh of the full scale Genesis spar. These later meshes contained approximately 1.6M nodes each. Figure 4 shows a foreshortened view of the surface mesh on the spar for a typical mesh with appurtenances.

In a typical simulation, the motion of the platform was calculated using the integral of the surface tractions on the spar and appurtenances at each time step. Platform motion is found by numerical integration of the equations of rigid body motion for the spar using the trapezoidal rule. The motion was confined to two degrees of freedom in the horizontal plane in the problems described here. The time step was kept constant in each simulation. Typically the time step provided between 50 and 100 steps for a complete period of oscillation of the spar.

Modeling Appurtenances

Initial CFD analyses modeled only the cylindrical hull and the strakes designed to disrupt the vortex formation. While these are obviously the key features, most spars have additional appurtenances such as the mooring chains, fairleads, pipes and anodes as seen in Figure 1 & 2. Furthermore, scale model experiments have shown that the presence of appurtenances can change VIM amplitudes. In order to improve confidence in the CFD modeling, a separate numerical investigation into the potential role of the mooring chains and pipes running down the upper half of the hull was undertaken at both full and model scale Reynolds numbers, *Re*~30e6 and ~3e5 respectively. In these studies, short sections of the spar were simulated with and without appurtenances, but without strakes, using DES. The appurtenances were simulated using either a fine mesh or a very course mesh. The fine mesh was such that it satisfied the general requirements for DES. The coarse mesh retained the treatment in the hull boundary layer of the fine mesh but used a very coarse mesh on the appurtenances. Thus the computational cost of modeling the appurtenances was an increase in the total number of nodes over a similar mesh without appurtenances by about 100% for a fine mesh with a number of appurtenances and about 20% for a course mesh of the same geometry. Note that in both cases we did not model the detailed geometry of the chains in the mooring system but rather replaced them with a pipe of the same frontal area.

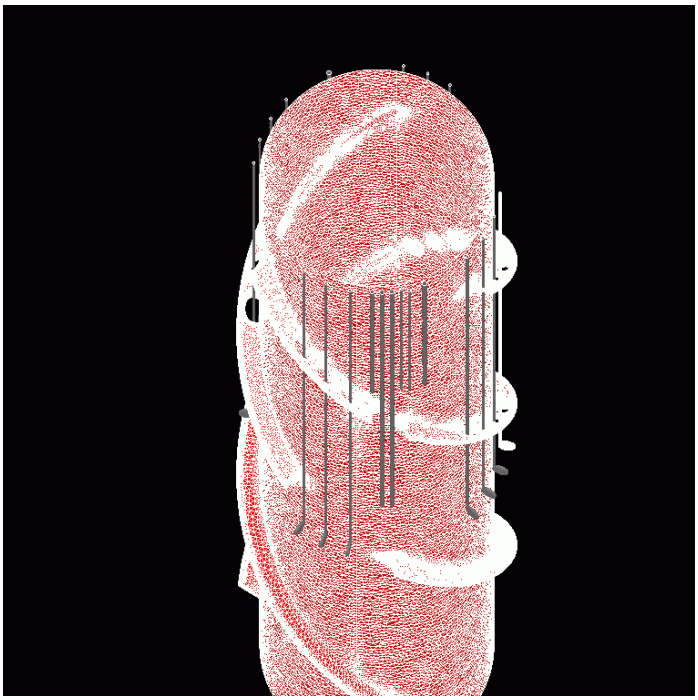

Figure 4 Surface mesh representing a spar platform with appurtenances shown in grey.

It was found from the simulations of the short cylinder sections that, in terms of the VIM of the spar section, the details of the mesh around the appurtenances made little difference in predicted response. Velocity and eddy viscosity profiles in the wake of the appurtenances were also similar for the two mesh types. However, the presence of appurtenances made a great deal of difference in the flow near the platform and may explain a lot of the effects of the appurtenances. Figure 5 shows contours of velocity magnitude from one of these simulations. Note the thick bands of low speed flow in the wake of the appurtenances.

Figure 6 shows a close up of the coarse mesh strategy for appurtenances that was used in the remainder of this study. Note that although surface element area on the appurtenance is

smaller than that on the spar itself, the relative size is much larger. The remainder of the model includes the details of the strakes which have pass-though holes for the fairleads and pipes and breaks at mid depth. These details also include fairleads, the exterior firewater piping and pipe models for the mooring chain. These features are expected to influence the flow around the spar as they are prominent and ubiquitous.

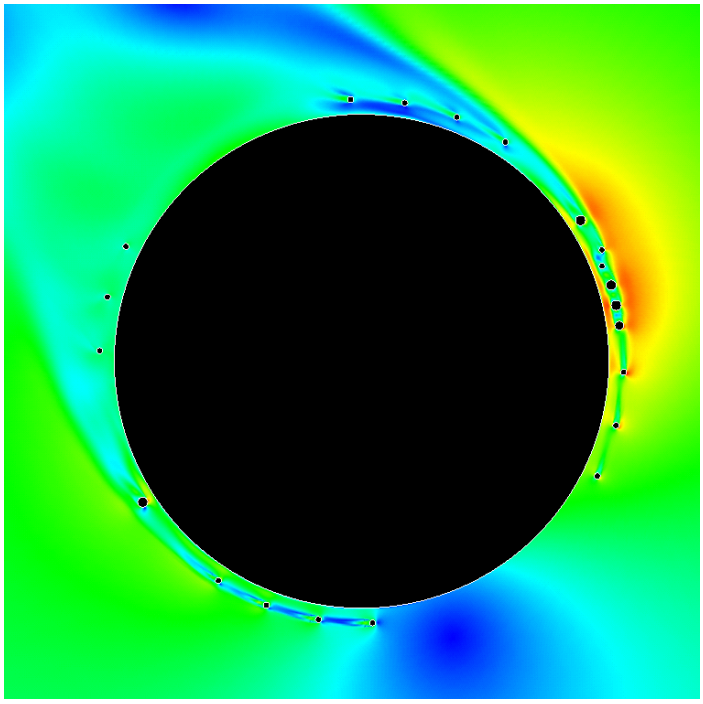

Figure 5 Influence of appurtenances on the flow around the platform as shown by velocity magnitude contours.

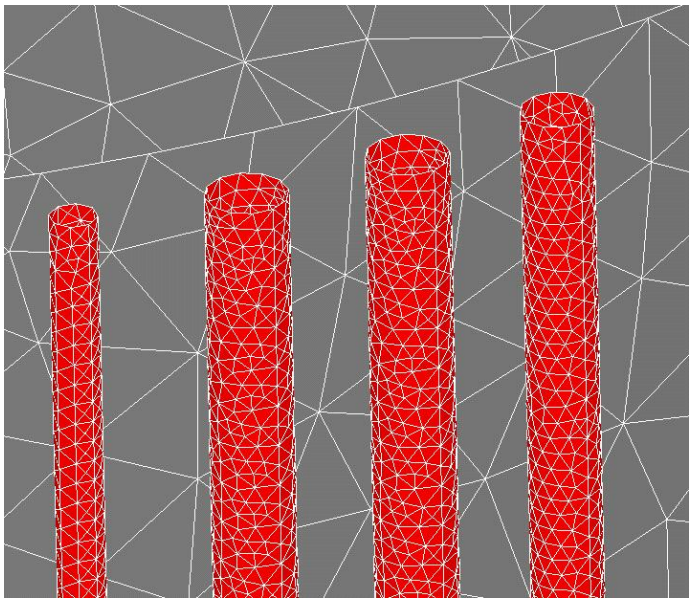

Figure 6 Close-up of appurtenance mesh made with course mesh strategy.

Uniform Flow Benchmarking

The Genesis model test program included an extensive series of experiments at different combinations of heading, current (tow) speed and mooring stiffness. Reynolds numbers and surface roughness were also varied. The experiments available for comparison here were performed at the MARIN facility in the Netherlands[1] in 1:46-scale giving a model spar hull diameter of 0.8m and a draft of 4.26m. It is well established that VIM, if it occurs, tends to be strongest when the natural frequency of vibration of the spar coincides with the vortex shedding frequency or at reduced velocities (U_{rn}) of about 6 or 7, which correspond to a Strouhal number (S_t) of a little less than 0.2. The model tests of Genesis all showed significant VIM in this region and plus a dependence on heading.

In the MARIN experiments, tests were run at varying Reynolds numbers by varying the mooring stiffness and tow speed, thus controlling both U_{rn} and *Re*. For the comparisons used here, we chose a series of tests with varying headings and a constant mooring stiffness of 725 N/m. The model mass was 2254 kg. A still water added mass coefficient of 1.1 yields a full scale natural period in surge and sway of 106 s and 15.5 s model scale. A nominal reduced velocity of 7 yields a current speed of 0.357 m/s and a model *Re* of 2.5e5. The surface roughness parameter was estimated as $k_s / D = 0.002$.

A series of simulations were run using the three dimensional mesh shown in Figure 4. Figure 7 shows an estimate of the maximum relative amplitude of cross-flow vibration *a/D* as a function of reduced velocity for the model shown in Figure 2 at 240 degree [6]. The computations are at

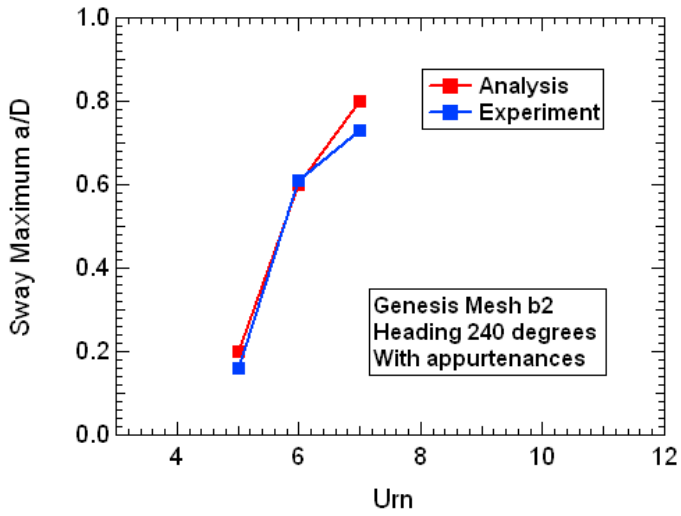

Figure 7 *a/D* versus reduced velocity Urn, uniform current model scale. The mesh includes all hull appurtenances, except for the anodes. This particular model test, unlike most others,

[1] Maritime Research Institute Netherlands – Depressurized Towing Tank

did not include the hull anodes. Hence the physical model and the numerical model were essentially identical. The reduced velocity trend is well represented.

Figure 8 shows the envelope of the maximum amplitude of cross-flow vibration *a/D* as a function of heading, extracted from all U_{rn} tests. The numerical maxima are estimated as $\sqrt{2}$ times the standard deviation of *a/D* for $U_{rn} = 7$. The CFD computations appear to be capturing the directional dependence of the hull geometry, justifying the addition of the appurtenances. Note that similar past experiments have shown that the VIM amplitude can change with the addition of appurtenances and large changes in surface roughness. Therefore care must be taken in projecting these results to full scale.

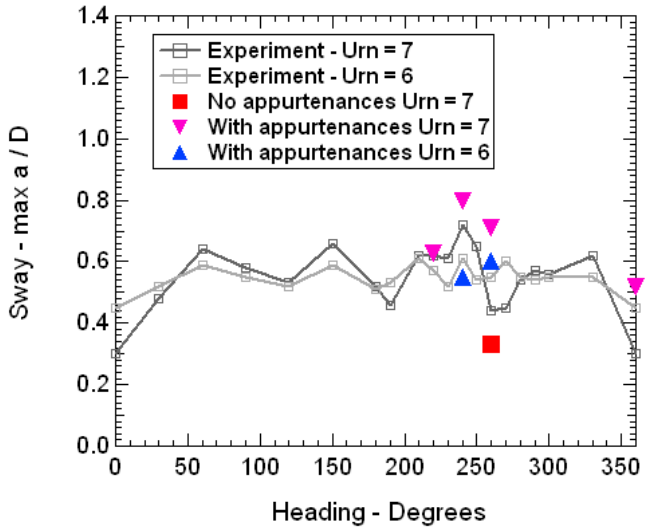

Figure 8 Spar VIM vs. heading at model scale in a uniform current profile.

The above results give us some confidence that the numerical model can duplicate the trends of the experiments. Unfortunately only a few full scale examples of VIM in a loop current have been recorded. Although the field data also showed large *a/D* (a maximum of 0.37), the field data is not readily compared with the scale model experiments because the field data current conditions are not well known and are thought to be strongly sheared. None the less, the assumption here is that CFD can be used to better understand how a spar design resists VIM in the model tests, to provide full scale *Re* estimates and finally test alternative experimental procedures.

CFD MODELING OF STRATIFIED FLOWS

Current Profiles

An important hydrodynamic design case in certain locations in the Gulf of Mexico involves a high velocity current shortly after the passage of a hurricane, referred to as the "inertial" current. Figure 9 shows this design hurricane current event along with a 100 year loop current profile. Note that the inertial current extends over the upper 1/3 of the spar while the water below is relatively quiet. These currents tend to be much shallower than the spar's draft so that model tests in a uniform current will not replicate the full scale flow. The associated waves for this case are less than those at the peak of the hurricane, but could result in significant mooring loads in addition to the VIM contribution. For this reason, the inertial current case could be controlling and needs to be examined critically. It is not obvious whether waves would have a significant effect on VIM amplitudes since their period is an order of magnitude shorter than VIM periods. This makes the computational load significantly larger due to the shorter time steps required. CFD studies have been performed with waves, but are not included in the present analysis.

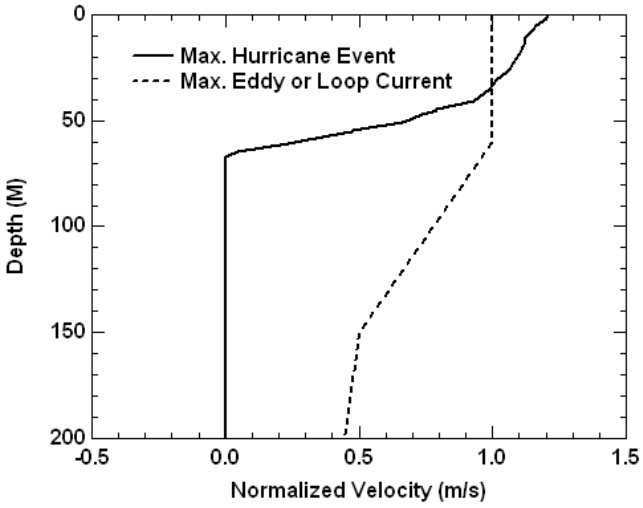

Figure 9 Example Gulf of Mexico 100 year loop and hurricane current profiles.

The inertial current is confined to the mixed layer where the temperature and salinity are relatively constant, respectively higher and lower than the quiescent water below. The characteristically sharp pyctocline traps the relatively warm, fresh current. The profile depth is stationary for the time period (hours) in question.

The physical or numerical modeling of the stratified currents requires the inclusion of buoyancy effects; hence the use of the Boussinesq approximation in equations 1 to 3 earlier. Froude scaling has been used to study smokestack plumes and similar problems, so a simple approach might be to use Froude scaling in a model basin. On the other hand, it is not clear that whether or not buoyancy will affect the flow around the platform. For example, is it sufficient to force a sheared flow in a model test using vanes or other means without adding the effects of density variations? Will Reynolds number effects be important? A better understanding of these questions can be obtained by substituting Froude scaled variables into Eqns. (1-3) as shown in Eq. (4-6). Here we assume we are using the same fluid and temperature range at all scales. The result implies that the Reynolds, Grashoff and Prantl numbers are important in scaling the flow as seen in Equations (4-6). The continuity equation is satisfied automatically and the momentum equation (5) will be conserved if the effect of changes in Re on τ_{ij} is small because Gr/Re^2 remains constant under these conditions. However, this is not likely at scale factors of interest and the last term in the energy equation does

not scale either because 1/RePr will change with scale factor. Thus, the simple forced sheared flow will not work if buoyancy effects are important in determining the vortex shedding of the platform.

It is not so easy to answer the question of the importance of buoyancy effects in forced convection. However, it is customary to assume that buoyancy effects are important in forced convective flows if the coefficient of the last term in (5) is on the order of 1 [7]. For flow velocities on the order of 1 m/s and temperature ranges of 10 C this is indeed the case, so we expect buoyancy effects may be important here.

$$\nabla \cdot u = 0 \tag{4}$$

$$\frac{Du}{Dt} = -\frac{1}{\rho}(\nabla p - \nabla \tau_{ij}) + \frac{Gr}{\mathrm{Re}^2}\Delta\Theta \tag{5}$$

$$\frac{D\Theta}{Dt} = \frac{1}{\mathrm{RePr}}\nabla^2\Theta \tag{6}$$

where

$$x = x / L; u = u / \sqrt{L}; ...$$

A final note on sheared currents should be mentioned here. Sheared currents in the ocean can exhibit a variety of instabilities some of which occur in the time and distance scales of interest here. In particular, Kelvin-Helmholtz and Helmboe [8] instabilities in a sheared current can give rise to traveling subsurface waves in between the warm upper layer and the cool lower layers of fluid. A rough condition for stability of this layer is based on the Richardson number,

$$R_i = g\Delta\rho\Delta h/(\rho\Delta u^2)$$

which represents the relative strength of buoyancy effects to vertical shear effects; Δu is the change in velocity over the depth of the shear layer represented by Δh. In general, a Ri of 0.25 or less is a condition for instability leading to the generation of internal waves [9]. At this time we don't know if these waves are important to VIM or not, so we assume that they may be important. Thus we don't attempt to suppress instabilities in the simulations and choose realistic current conditions based on field observations. The sheared current modeled later in this paper is based on field data of velocity, salinity and temperature which was used to create the velocity profile shown in Figure 9 and associated density profiles. Calculation of the Richardson number vs. depth for this current gives values of 0.5 or less in much of the flow so internal waves may occur. Note that the current direction is assumed constant and unidirectional.

Another concern in the numerical simulations is the diffusivity of salinity and temperature in the flow, especially around the platform. One could track both these scalars independently and might be tempted to do so as the molecular diffusivity for salt is much higher than that for heat. However, recent work [10] shows that even for Reynolds numbers orders of magnitude less than those of interest here, the diffusion rates are dominated by turbulent mixing and are essentially the same. For simplicity we assume that the transport effects are the same for salinity and temperature and that they can be treated as a single advected scalar.

One of the primary virtues of CFD modeling is the ability to visualize the flow details and compare different flows and geometric details. Figure 10 illustrates the difference in the flow about the spar in a uniform and in a sheared current.

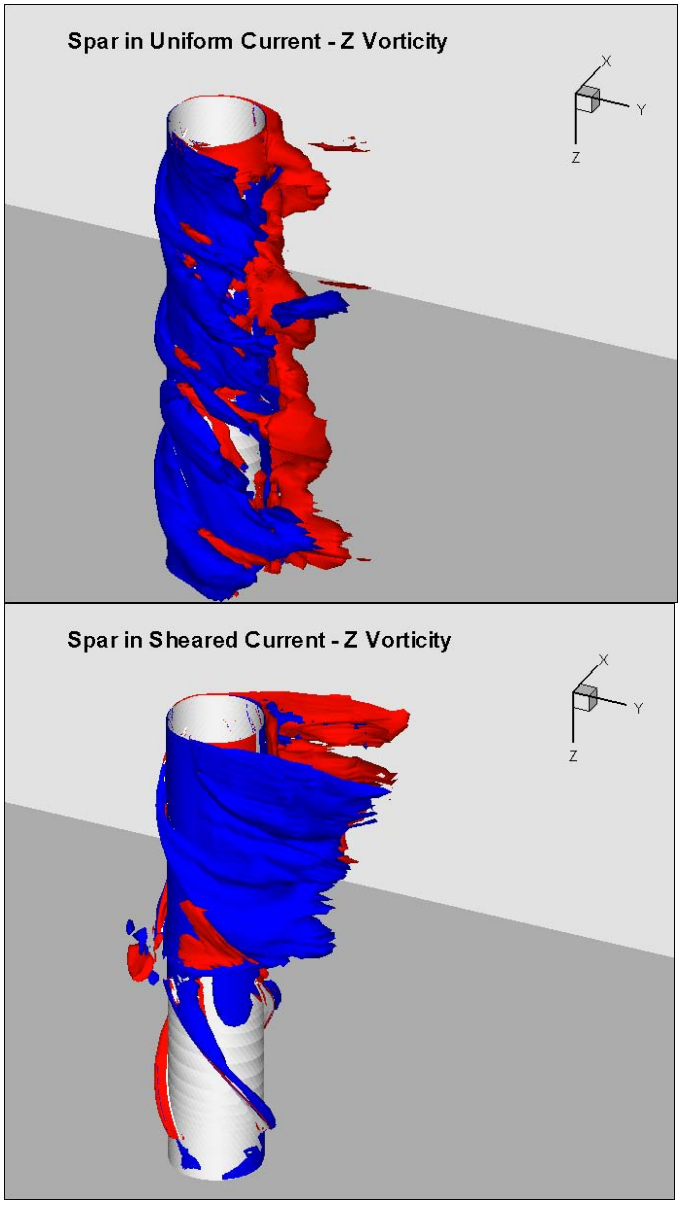

Figure 10 Flow in uniform and sheared current

Animations clearly reveal differences in the coherence of the vorticity in the neighborhood of the thermocline. It is desirable to benchmark these computations against measurements if at all possible. Few such experiments have been attempted and their design posses some interesting questions.

Experiments at Small Scales

Scale model experiments are typically performed in tow tanks or basins where attempting to add fluid stratification would be at best challenging. An obvious question is whether a surface jet would be a suitable proxy for the stratified case, since it would be relatively easy to engineer? Although appealing, this arrangement leaves out the potentially important full scale effect of buoyancy. Buoyancy plays a vital role in the development and stability of the shear current as discussed widely in the literature; see Refs. [8-11]. The potential importance is clear if one tries to maintain a sheared current in a water channel without buoyancy effects. Flow introduced at the inlet top of the channel quickly diffuses though the channel and the current dissipates. The numerical modeler quickly discovers the same effect if he attempts to model an ocean current without introducing buoyancy effects.

It has been proposed to overcome this problem through the use of a divided water basin in which a high flow rate is introduced in the upper part of the tank while quiet water is maintained below. For example the spar model could be placed a hole in the raised false floor available in one of the test basins. CFD simulations of this geometry and profiles measured in the basin suggest that if the model is placed reasonably close to the leading edge of the hole, the desired profile can be achieved. A CFD analysis shows that dispersion and 3D vortices rapidly grow downstream, across a representative hole as see in Figure 11.

Two additional considerations remain. One is the level of ambient turbulence generated by the current pumps. Presumably this can be controlled to be in an acceptable range and the issue was not addressed in the computational model. The second consideration is the impact on vortex coherence, i.e. 3D effects, due to the lack of stratification. In the case of very strong stratification, the primary vertical VIM vortices would be expected to terminate at the density interface like they do at the free surface. As the stratification is reduced, this wall effect weakens and coherence of these strong vertical vortices presumably decreases. In the absence of any stratification, the strength of the vortices would be lowest and therefore the test would be non-conservative. The VIM amplitude would not be as large as in a stratified flow where the profile is more two-dimensional. This effect can be investigated by simply reducing the stratification in the CFD simulation. It was decided to check the full scale vs. model scale responses first to see if the issue was potentially critical. The assumption here is that CFD is capable of accurately predicting trends, as demonstrated in the uniform current studies above. Hence the simulations should give an indication of the potential degree of non-conservativeness of the proposed small scale experiment.

Stratified Flow Modeling - Prototype vs. Model Scale

Here we compare our full scale CFD estimates of VIM in a sheared profile with the proposed hole-in-the-floor model test configuration. One objective is to develop a feel for the degree of accuracy of model scale tests in a sheared, but un-stratified, profile.

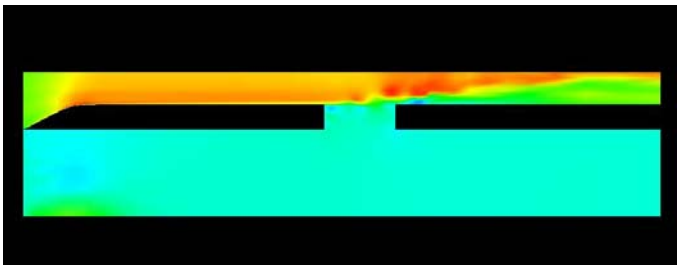

(a)

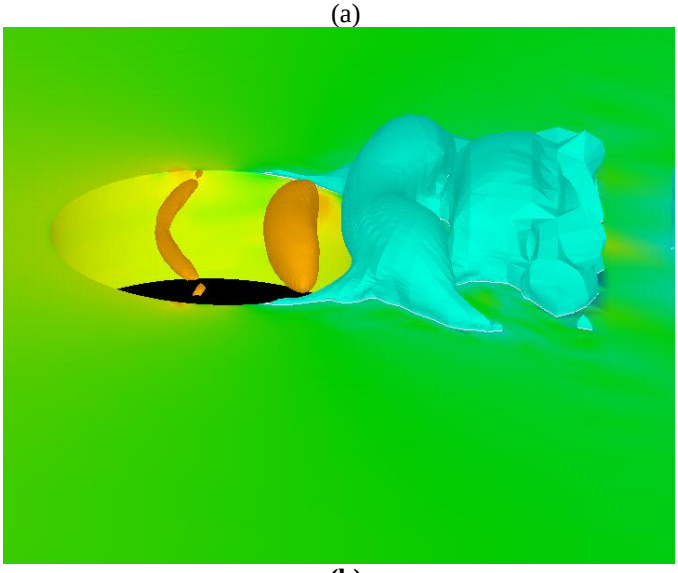

(b)

Figure 11 Contours of horizontal velocity at the center plane of the basin (a) and pressure iso-surfaces around the hole showing pressure oscillations (b).

The full scale case is the hurricane inertial condition with stratification, but without waves or anodes on the spar platform. The flow on the platform shows the strong highly sheared current coming from the left as shown in the contour plot of velocity magnitude in Figure 12. The contours indicate that the warm current is pushed downward as it encounters the spar so that a region of higher velocity is found in front of the spar to a depth about 50% greater than the current depth (~65 m). On the other hand, buoyancy does seem to have an effect on the flow as the intrusion of the warm current is limited to a fraction of the spar draft. Reynolds number effects were investigated by computing the same stratified flow at model scale. The sway amplitude a/D was slightly smaller, but otherwise the response was similar.

In the model scale case, we have placed the same spar mesh in the false floor of the basin to create a similar velocity magnitude contour plot; see Figure 13. Note the edges of the hole in the false floor at the sides of the figure. In this simulation the fluid above and below the false floor are assumed to have the same temperature and density. The velocity magnitude contours in Figure 13 contrast sharply with those of Figure 12. In the latter figure, the intrusion of the upper flow into the quiet lower flow is much more pronounced.

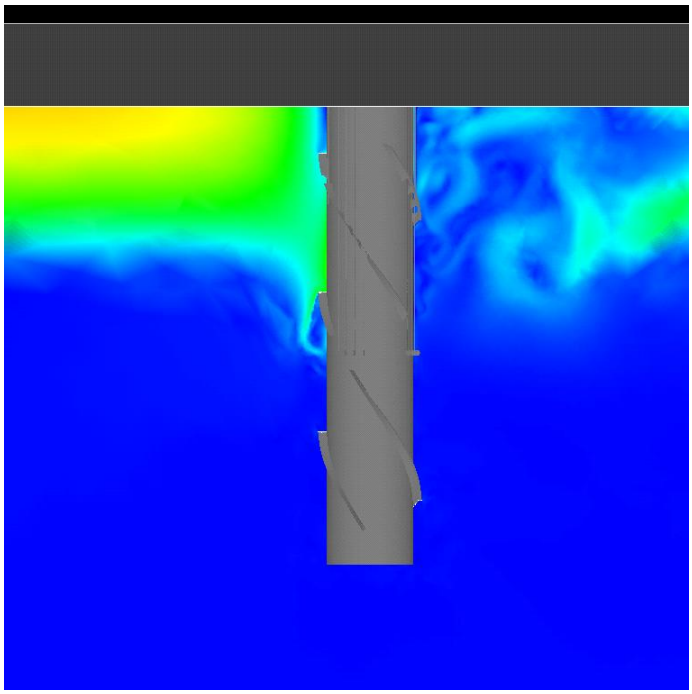

Figure 12 Predicted velocity magnitude contours on center plane for a full scale spar in hurricane currents

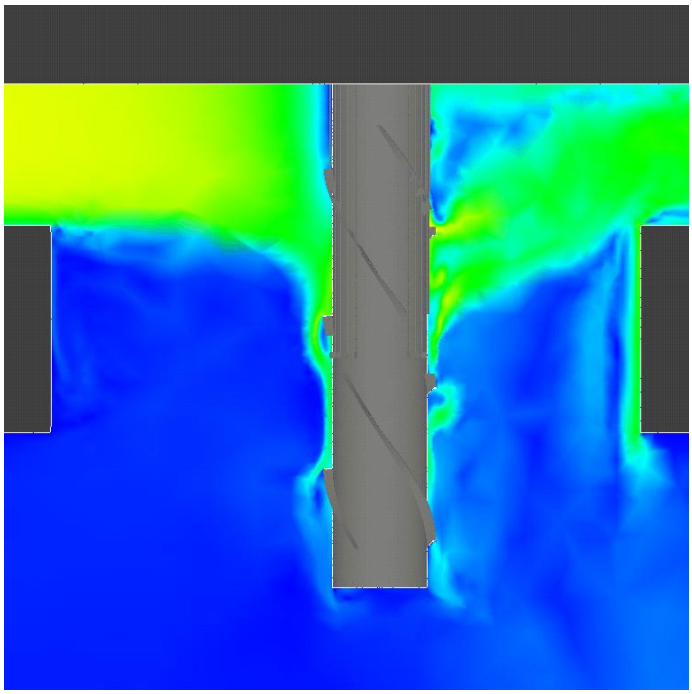

Figure 13 Predicted velocity magnitude contours for a 1:46-scale spar in a divided tank without buoyancy effects

Also, when we examined the two flow simulations we found differences in the vortex structures predicted behind the two spars. This leads us to conclude that buoyancy may have an effect on the flow around spars in a strongly sheared current.

The differences in the vertical mixing appear to also have an effect on the surge and sway amplitudes. We compare surge and sway amplitude for the simulation of a full scale spar in a hurricane current with the sway amplitudes predicted for the basin experiment in Figure 14. In this graph we show a/D. The simulation indicates that the basin experiment will produce VIM sway amplitudes that will be somewhat lower than those that will occur in the field. Also, the character and trajectories of the two motions will be different. Hence for this hull geometry, scale model tests without buoyancy would appear to be non-conservative in that the sway motion could be under predicted.

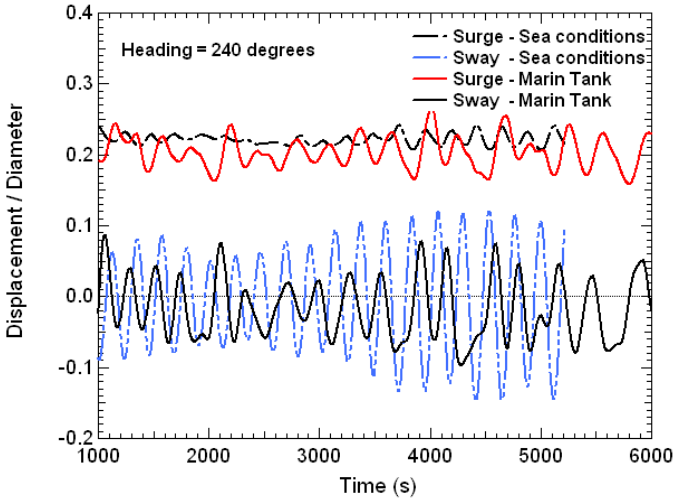

Figure 14 Comparison of a/D computed for full scale and model scale spars.

SUMMARY & CONCLUSIONS

The overall objective of the work described here is to examine the effectiveness of both CFD and split tow tanks in the prediction of spar platform VIM in sheared currents. We identified a series of modeling and prediction considerations. Important issues are the question of the appropriate type turbulence model, the mesh resolution required and other CFD modeling techniques. We chose to use detached eddy simulation (DES) with wall functions along with careful planning of the mesh in order to capture as many details of the flow as possible and to minimize computational cost. To this end, an auxiliary study of short vertical sections of the spar was made of the mesh refinement required in the modeling of appurtenances. It was found that for the geometry of the pipes and chains used on the exterior of Genesis, a relatively coarse mesh produced similar overall flow and load distributions on the main spar surface and hence should produce similar VIM response. These allowed significant economies in simulating the overall platform. Several mesh refinements were used up to a maximum of 1.6M nodes. Meshes were created of model scale spars in uniform flows and in a horizontally split tow tank and in full scale.

A second important issue is the prediction of VIM and validation of CFD in this application. Although the study described here cannot be considered definitive, several one-to-one comparisons were made of CFD simulations with tow tank

experiments. These produced generally good agreement in terms of overall motions and frequencies as well as most trends.

A final important question arising from the physics of the problem is whether or not buoyancy effects need to be included numerically and in physical simulations. Although it is well established that buoyancy effects are important in the maintenance of sheared currents it was not clear whether or not these effects will influence the vortex structure around a full scale or model scale spar. We developed methods to include density changes and hence buoyancy effects due to both temperature and salinity variations and examined the effects of buoyancy through CFD simulations. These simulations suggest that buoyancy does affect the vortex structure around the spar platform. We directly compared VIM predicted in full scale using the density and velocity profiles measured in the field with predictions of model experiments using a horizontally split tow tank. This comparison suggests that the split tank would produce VIM with an amplitude somewhat smaller than those expect in the field unless a density gradient was introduced in the tank. However, the effectiveness of such an approach was not investigated here.

Finally, it should be noted that a good many questions remain and further development is needed to bring the techniques developed here into general use. The simulation of turbulence effects at the high Reynolds numbers found in both the scale model experiments and especially in full scale applications requires further study. The effects of small appurtenances and boundary layer modeling need to be studied further and better understood. Also, although not reported here, the authors have included the simulation of waves along with sheared currents so that the interaction of these sea conditions is another area of potential study.

ACKNOWLEDGMENTS

The authors wish to acknowledge the contributions of Tim Finnigan of ChevronTexaco for his helpful suggestions and Greg Buley for the mesh generation.

REFERENCES

[1] Glanville, R.S., Halkyard, J.E. , Davies, R.L., Steen, A. and Frimm, F., 1997, "Neptune Project: Spar History and Design Considerations", Offshore Technology Conference, Houston, OTC-8382

[2] Sirnivas, S., Halkyard, J. E. and Finn, L. , 2003, "SPARs - Lessons Learned", 1st PetroMin Deepwater Conference

[3] Spalart, P. R. and Allmaras, S. R., 1992, "A one-equation model for aerodynamic flows," AIAA 92-0439

[4] White, F. M., 1991, *Viscous Fluid Flow*, 2nd ed., McGraw Hill Boston

[5] Jansen, K. E., Whiting, C. and Hulbert, G., 2000, "A generalized-alpha method for integrating the Navier-Stokes Equations with a stabilized finite element method," *Computer Methods in Applied Mechanics and Engineering*, **in press**

[6] Mercier, R.S. and Ward, E.G., 2003, Proceedings of MMS/OTRC Workshop "Spar Vortex-Induced Motions", October 22-24 (2003)

[7] Kreith, F., 1965, *Principals of Heat Transfer*, International Textbook Company pp. 358

[8] Smyth, W.D. and Winters, K.B., 2002, "Turbulence and mixing in Holmboe waves", J. Phys. Oceanography, (2 Oct.)

[9] Stewart, R. H., 2004, *Introduction to Physical Oceanography*, Texas A& M University (2004) pp 129-132

[10] Smyth, William, J. D. Nash, and Moum, J. N. , 2004, "Differential Diffusion in Breaking Kelvin Helmholtz billows", J. Physical Oceanography (22 Nov.)

[11] Skyner, D. J., Created, C. A. and Eason, W.J., 1992, "The internal kinematics of steep waves on sheared current", University of Edinburgh Offshore Technology Report, OTH 92 366

